Journal of Molecular Liquids 400 (2024) 124505

Contents lists available at ScienceDirect

Journal of Molecular Liquids

journal homepage: www.elsevier.com/locate/molliq

Efficient and selective absorption of NH_3 by supramolecular OHP[5]-based ternary deep eutectic solvents

Wen-Qiang Gong, Ming-Shuai Sun *, Jun Li, Qiu-Ping Gong, Yu-Xuan Fu, Yan Zhou, Duan-Jian Tao *

National Engineering Research Center for Carbohydrate Synthesis, Key Laboratory of Fluorine and Silicon for Energy Materials and Chemistry of Ministry of Education, College of Chemistry and Chemical Engineering, Jiangxi Normal University, Nanchang 330022 China

ARTICLE INFO

Keywords:
NH_3 capture
Deep eutectic solvent
Pillar[5]arene
High selectivity

ABSTRACT

Developing an efficient absorbent for selective ammonia capture is of significant importance in the recovery and utilization of ammonia resources. Herein, a series of supramolecular-based ternary deep eutectic solvents (DESs) was designed and prepared using per-hydroxy pillar[5]arene (OHP[5]) and ethylamine hydrochloride as the key components. It is found that the supramolecular-based ternary DES EaCl-Gly (1:2)-6% OHP[5] could be employed as an efficient absorbent for reversible absorption of NH_3. The NH_3 uptake capacity reached 2.39 mmol/g and 10.84 mmol/g at 298.2 K under the pressure of 10 kPa and 100 kPa, respectively. Meanwhile, a higher NH_3/CO_2 selectivity (84) was obtained at 298.2 K and 100 kPa owing to the low solubility of CO_2 in EaCl-Gly (1:2)-6% OHP[5]. The results of ^1H NMR and FTIR spectra further clarified the absorption mechanism of NH_3 by EaCl-Gly (1:2)-6% OHP[5]. Accordingly, the chemical absorption and physical dissolution capacity of NH_3 in EaCl-Gly (1:2)-6% OHP[5] were calculated on the basis of isotherm data and thermodynamic equations. This study offers a promising application of pillar[5]arene to form supramolecular-based DESs for efficient NH_3 absorption.

1. Introduction

As an important industrial raw material, ammonia gas (NH_3) is widely used in industry production. For example, nitrogen fertilizer, urea, sulfonamide and ammonium salts are synthesized using ammonia gas as raw materials [1–3]. In addition, the content of hydrogen atoms in NH_3 can reach 17.6 wt%, and NH_3 is easier to liquefy than H_2, making it a great advantage for storage and transportation. Therefore, NH_3 may have better application prospects than H_2 in the energy field [4–6]. On the other hand, NH_3 is one of the main atmospheric pollutants. A large amount of NH_3 released in the process of chemical production has caused serious environmental pollution. For example, a large amount of NH_3 emissions will cause the problem of exceeding the standards for PM2.5, and NO_x produced by NH_3 in the oxidation process will further lead to the occurrence of nitric acid rain. These would cause great damage to the environment and human physical health [7,8]. Therefore, it is important to develop a type of new absorbent or adsorbent with high efficiency and selectivity for NH_3 separation.

At present, NH_3 in the tail gas is usually removed by scrubbing with water or water solution of inorganic acid [9–11]. However, a large amount of ammonia wastewater is produced during the NH_3 removal processes, and the treatment of ammonia wastewater is very complex and tedious. In order to efficiently separate and purify NH_3 from the tail gas, various novel liquid solvents such as protic ionic liquids [12–15], hydroxyl-functionalized ionic liquids [16–18], metal-based ionic liquids [19,20], and metal-based DESs [21–23] have been reported for efficient absorption and purification of NH_3. For example, Ma et al. designed an ImCl + Gly DES for reversibly capturing NH_3 with a capacity of 12.93 mmol/g at 298.2 K and 101.3 kPa through a hydrogen bonding interaction. However, the performance of the ImCl + Gly DES for NH_3 absorption was down 16 % after five NH_3 absorption–desorption cycles [24]. Wang et al. also developed a metal-based ionic liquid $[Bmim]_2[CuCl_4]$ for achieving a NH_3 uptake of 10.1 mmol/g through a coordination interaction, but about 20 % captured NH_3 could not be desorbed and released from the complex of $[Bmim]_2[CuCl_4] + NH_3$ after 5 cycles [19]. These progresses show that the interaction of metal-based ionic liquids or DESs with NH_3 molecules seems a bit strong. Therefore, the screening of advanced absorbents with good reversibility for efficient

* Corresponding authors.
E-mail addresses: mingshuaisun@jxnu.edu.cn (M.-S. Sun), djtao@jxnu.edu.cn (D.-J. Tao).

https://doi.org/10.1016/j.molliq.2024.124505
Received 17 December 2023; Received in revised form 12 March 2024; Accepted 15 March 2024
Available online 16 March 2024

absorption and purification of NH_3 is still in high demand.

Pillar[n]arenes are a class of macrocyclic supramolecular compounds with columnar structures and multiple modifiable chemical sites [25,26], which exhibit good performance in gas adsorption. In particular, per-hydroxy pillar[5]arenes (OHP[5]) possessing many phenol hydroxyl groups have a good potential to capture NH_3 via a acid-base interaction. Moreover, the use of liquid absorbents for NH_3 capture have the advantages of considerable solubility, continuous operation and low cost. It is a good strategy to dissolve OHP[5] in DES and reconstruct a type of new liquid absorbents. [27,28] Then the design and preparation of liquid absorbents composed of OHP[5] are helpful and expected to achieve the effective capture and recovery of NH_3.

In this study, a series of supramolecular OHP[5]-based ternary DESs were designed and applied for reversible and efficient absorption of NH_3. The NH_3 absorption capacity and reversibility could be controlled by adjusting the species composition and molar ratio. Moreover, the proton nuclear magnetic resonance (^{1}H NMR) spectra and Fourier transform infrared (FTIR) spectra of supramolecular OHP[5]-based ternary DESs before and after NH_3 capture were tested to study the interaction mechanism. The thermodynamic analysis was further carried out to realize the NH_3 absorption behavior. In addition, the recyclability of supramolecular OHP[5]-based ternary DESs in the NH_3 absorption–desorption process was also investigated.

2. Experimental section

2.1. Experimental materials

Ethylamine hydrochloride (EaCl, 98 %), urea (99 %), acetamide (AA, 99 %), glycerol (Gly, 99 %), 1,4-dimethoxybenzene (99 %), boron tribromide (99 %), boron trifluoride diethyl etherate (98 %), paraformaldehyde (95 %), chloroform (99.5 %), 1,2-dichloroethane (99.5 %), and dichloromethane (99.5 %) were purchased from Shanghai Macklin Biochemical Co., Ltd. Ammonia (NH_3, 99.99 v/v%) and carbon dioxide (CO_2, 99.99 v/v%) were purchased from Jiangxi Huahong Special Gas Co., Ltd. All reagents were used directly without further treatment.

2.2. Synthesis of OHP[5]

The synthesis procedure of OHP[5] was carried out according to the method previously reported [29]. The first step is the synthesis of precursor dimethoxypillar[5]arene (DMP[5]). 1.38 g of 1, 4-dimethoxybenzene and 0.93 g of paraformaldehyde were added to 20 mL solution of 1, 2-dichloroethane. After stirring at room temperature for 30 min, 1.25 mL of boron trifluoride ether was added to the reaction solution. The reaction solution was stirred for 30 min at 303.2 K. After that, water was added to quench the reaction. Finally, DMP[5] was separated and obtained by column chromatography (petroleum ether: dichloromethane = 1:3).

For the synthesis of OHP[5], 0.5908 g of DMP[5] and 5.010 g of boron tribromide were added into 30 mL of chloroform. Then the solution was stirred continuously at room temperature for 72 h. After that, 30 mL of water was poured into the reaction solution to remove excess boron tribromide and thereby to obtain white precipitate. The white precipitate was washed with chloroform and HCl (0.5 M). As a result, the white powder OHP[5] was dried and obtained under vacuum for 12 h. The yield of OHP[5] was 54 %.

2.3. Preparation of OHP[5]-based ternary DESs

As shown in Scheme 1, all the OHP[5]-based ternary DESs were prepared by mixing OHP[5] and EaCl with one of Gly, Urea, and AA. In a typical run, EaCl and Gly were mixed with a molar ratio of 1:2 to obtain the EaCl-Gly (1:2) DES at 353.2 K for 1 h. After that, 6 wt% OHP[5] was added to the EaCl-Gly (1:2) DES and stirred for another 1 h. As a result, the homogenous liquid was obtained and denoted as EaCl-Gly (1:2)-6% OHP[5]. The synthetic procedures of EaCl-AA (1:1)-6% OHP[5] and EaCl-Urea (1:1)-6% OHP[5] was according to that of EaCl-Gly (1:2)-6% OHP[5].

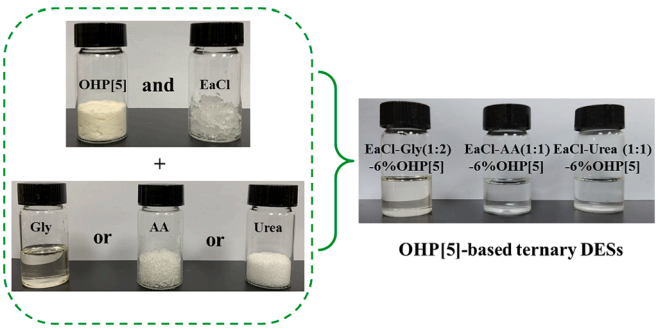

Scheme 1. Schematic illustration for the synthesis of supramolecular OHP[5]-based ternary DESs.

2.4. Characterizations

The ^{1}H and ^{13}C NMR spectra of supramolecular OHP[5]-based ternary DESs were obtained from 400 MHz Bruker Avance III spectrometer. The density of supramolecular OHP[5]-based ternary DESs were determined by Anton Paar DMA 4500 M densitometer. The viscosity of supramolecular OHP[5]-based ternary DESs were tested on Brookfield DV II + Pro viscometer. The thermal stability of supramolecular OHP[5]-based ternary DESs were examined by thermogravimetric analyzer (PerkinElmer Diamond TG/DTA) under N_2 atmosphere. The FTIR spectra of supramolecular OHP[5]-based ternary DESs were recorded by A Nicolet 6700 spectrometer.

2.5. NH_3 absorption

The experimental data of NH_3 absorption were obtained using a self-made experimental device, which is consistent with our previous work [30]. The specific experimental devices and processes are described in the supplementary data (Figure S1). The gas absorption capacity of supramolecular OHP[5]-based ternary DESs were obtained by calculating the pressure changes in the two gas chambers before and after NH_3 absorption. For the cycle performance test, the OHP[5]-based ternary DES loaded with saturated NH_3 was desorbed for 2 h under vacuum at 353.2 K, and then the regenerated OHP[5]-based ternary DES was used for the next NH_3 absorption experiment.

3. Results and discussion

3.1. Characterization

The structure of DMP[5] and OHP[5] were verified by ^{1}H NMR and ^{13}C NMR spectra, as shown in Figures S2-5. The results confirmed the successful synthesis of OHP[5], which is consistent with the structure reported in the literature. Moreover, Fig. 1 shows the thermogravimetric curves of OHP[5]-based ternary DESs in the temperature range from 323.2 to 1073.2 K under N_2 atmosphere. Thermal decomposition temperatures sequence of OHP[5]-based ternary DESs were as follows: EaCl-Urea (1:1)-6% OHP[5] > EaCl-Gly (1:2)-6% OHP[5] > EaCl-AA (1:1)-6% OHP[5]. The thermal decomposition temperatures of the three OHP[5]-based ternary DESs were all above 400 K, showing that they have good thermal stability in the NH_3 absorption–desorption cycles. And the melting points of three OHP[5]-based DESs were tested, as shown in Figure S10. The melting point of EaCl-Urea (1:1)-6% OHP[5] is about 278.5 K. But EaCl-Gly (1:2)-6% OHP[5] and EaCl-AA (1:1)-6% OHP[5] have not found their melting points, which may be due to their

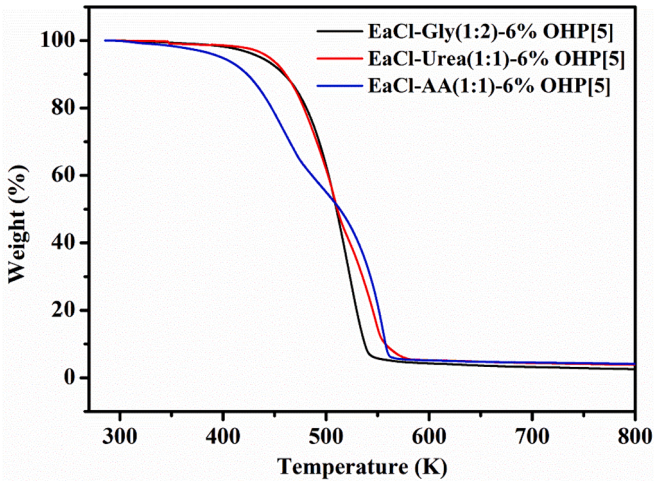

Fig. 1. TGA curves of OHP[5]-based ternary DESs.

amorphous structure.

3.2. Physical properties of OHP[5]-based ternary DESs

The density and viscosity of OHP[5]-based ternary DESs are the essential basic data of NH_3 absorption process. Fig. 2 shows the density and viscosity test results of three OHP[5]-based ternary DESs at different temperatures. It is obvious that the density of three OHP[5]-based ternary DESs decreased linearly with increasing temperature ranges of 293.2 ~ 353.2 K, while their viscosity values showed an exponentially decreasing trend at 313.2 ~ 353.2 K. And the viscosity of EaCl-Gly (1:2)-6% OHP[5] was lower than 75 cP at 313.2 K, which means that the mass transfer resistance of its absorption process is extremely low. Moreover, the density and viscosity values of three OHP[5]-based ternary DESs were fitted according to equations 1 and 2. The corresponding fitting parameters are listed in Table S1 in the supplementary data.

$$\rho = A + BT \tag{1}$$

$$\eta = \eta_0 * e^{\frac{D}{T-T_0}} \tag{2}$$

3.3. NH_3 absorption performance

Firstly, the content of OHP[5] in the absorbent was screened. With the increase in OHP[5] content from 2 % to 6 %, the NH_3 absorption capacity of EaCl-Gly (1:2)-6% OHP[5] also increases. When the mass percentage of OHP[5] is greater than 6 %, a homogeneous liquid cannot be formed. Therefore, the mass percentage of OHP[5] was selected as 6 %. In order to evaluate the absorption performance of NH_3, the absorption isotherms of NH_3 on three OHP[5]-based ternary DESs were measured at 313.2 K, as shown in Fig. 3. The results indicated that EaCl-Gly (1:2)-6% OHP[5] exhibited higher NH_3 absorption capacity (6.87 mmol/g) compared to EaCl-Urea (1:1)-6% OHP[5] (4.95 mmol/g) and EaCl-AA (1:1)-6% OHP[5] (4.64 mmol/g). The difference in NH_3 absorption capacity on three OHP[5]-based ternary DESs may be attributed to the fact that glycerol (Gly) contains more hydroxyl functional groups than urea and acetamide (AA). A more stable hydrogen bond network in EaCl-Gly (1:2)-6% OHP[5] contributes its higher NH_3 absorption capacity.

Subsequently, the NH_3 absorption rate of EaCl-Gly (1:2)-6% OHP[5] was investigated using pseudo-first-order kinetic (Eq. S1) and pseudo-second-order kinetics model fitting (Eq. S2) were further performed on the relevant NH_3 experimental data [31]. As shown in Fig. 4a, the NH_3 absorption equilibrium in EaCl-Gly (1:2)-6% OHP[5] can be reached within 5 min. This fast NH_3 absorption rate results from the low viscosity value of EaCl-Gly (1:2)-6% OHP[5] along with a relatively low gas mass transfer resistance during the absorption process. Furthermore, the fitting curve showed a high correlation ($R^2 > 0.98$) with the NH_3 absorption data. However, the pseudo-second-order kinetic model used to describe the NH_3 absorption process has an obvious deviation. For example, the fitting values and experimental values of NH_3 absorption capacity at 1 min are 6.9 and 8.1 mmol/g, respectively. And the fitting value of the NH_3 absorption capacity is significantly greater than the experimental value after 5 min. Compared with the correlation coefficient ($R^2 = 0.98$) of the pseudo-first-order kinetic model, the correlation coefficient ($R^2 = 0.96$) of the pseudo-second-order kinetic model is smaller. Therefore, pseudo-second-order kinetic models are not suitable

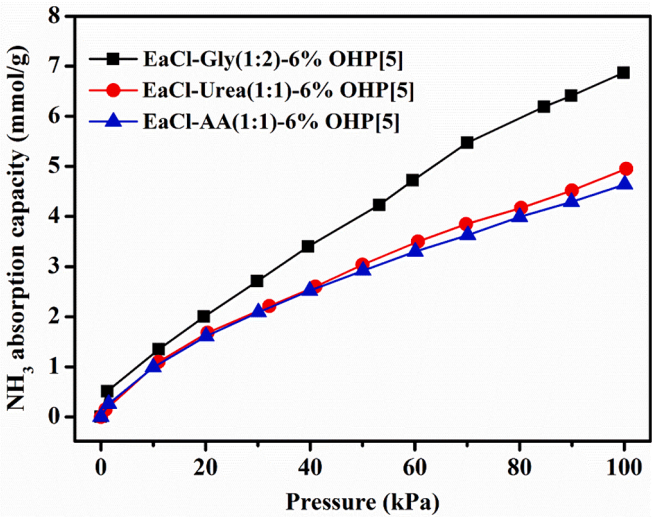

Fig. 3. NH_3 absorption isotherms in EaCl-Gly (1:2)-6% OHP[5] (■), EaCl-Urea (1:1)-6% OHP[5] (●), and EaCl-AA (1:1)-6% OHP[5] (▲) at 313.2 K.

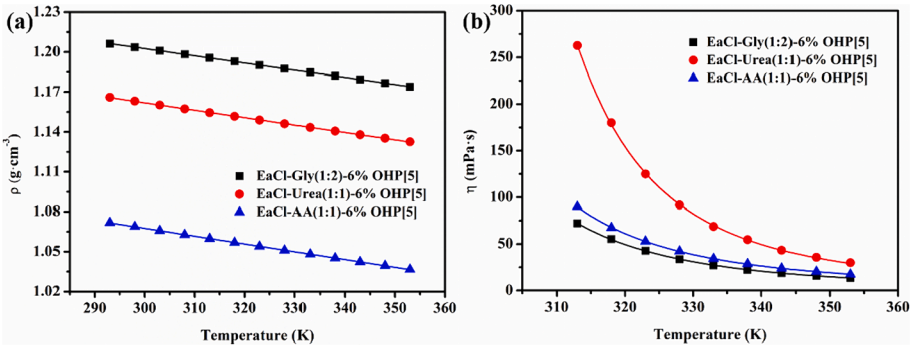

Fig. 2. Densities (a) and viscosities (b) of EaCl-Gly (1:2)-6% OHP[5] (■), EaCl-Urea (1:1)-6%v (●), and EaCl-AA (1:1)-6% OHP[5] (▲) at different temperatures.

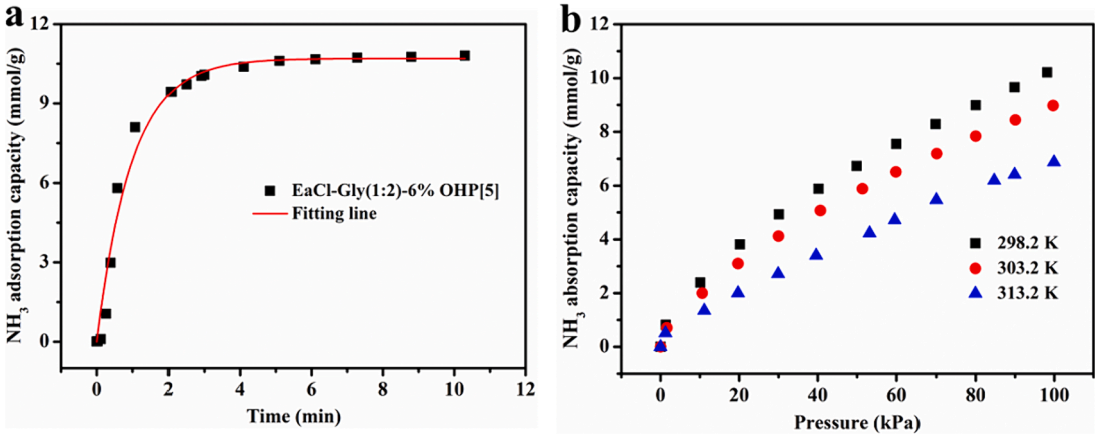

Fig. 4. (a) Pseudo-first-order kinetic model of NH_3 absorption on EaCl-Gly (1:2)-6% OHP[5] and (b) absorption of NH_3 in EaCl-Gly (1:2)-6% OHP[5] at different temperatures.

to describe the absorption process. The relevant kinetic model fitting parameters are also shown in Table S2 in the supplementary data.

The influence of temperature and NH_3 partial pressure on the NH_3 absorption performance of EaCl-Gly (1:2)-6% OHP[5] was further studied, as shown in Fig. 4b. When the temperature increased from 298.2 to 313.2 K, the NH_3-saturated absorption capacity in EaCl-Gly (1:2)-6% OHP[5] decreased from 10.8 to 6.9 mmol/g. This implies that the absorption of NH_3 by EaCl-Gly(1:2)-6% OHP[5] is an exothermic process. Moreover, the NH_3 absorption capacity of EaCl-Gly (1:2)-6% OHP[5] enhanced with the increase of NH_3 partial pressure, indicating that a higher pressure is beneficial for NH_3 capture. Notably, the NH_3 absorption isotherm of EaCl-Gly (1:2)-6% OHP[5] had an obvious nonlinear increase at the lower partial pressures of 0 ~ 20 kPa, whereas a linear increase in NH_3 absorption uptake was observed in the partial pressure range of 20–100 kPa. This suggests that there might exist two kinds of absorption interaction (chemical absorption and physical dissolution) between OHP[5]-based ternary DESs and NH_3 molecules.

3.4. Comparison of OHP[5]-based DESs with other absorbents in the literature

The NH_3 absorption performance of supramolecular OHP[5]-based ternary DESs and other liquid absorbents in the literatures were collected and listed in Table 1. It is found that the addition of OHP[5] can obvious improve the NH_3 absorption performance by comparing supramolecular-based ternary DESs (entries 1–3) and binary DESs (entries 4–6). For example, the absorption capacity of EaCl-Gly (1:2)-6% OHP[5] on NH_3 could reach as high as 2.39 (10 kPa) and 10.84 mmol/g (100 kPa), while the NH_3 absorption capacity on EaCl-Gly (1:2) was only 1.59 (10 kPa) and 9.34 mmol/g (100 kPa) at 298.2 K. Moreover, the NH_3 absorption performance of supramolecular-based ternary DESs are superior to tradition ionic liquids and DESs (entries 10–14). Although some functionalized ILs and DESs (entries 7–9 and 15–17) show higher NH_3 absorption capacity, the NH_3 absorption performance loss in their absorption–desorption cycles cannot be ignored. For example, ChCl + TetrZ + EG (3:7:14) DES lost 24 % of the saturation NH_3 capacity after 6 cycles. 3,4-DHBA + EG (1:3) had a 13 % loss of the saturation NH_3 absorption capacity after five cycles.

3.5. NH_3/CO_2 absorption selectivity

It is known that the NH_3-containing exhaust gas often contains CO_2 and N_2. Therefore, the absorption of CO_2 and N_2 by EaCl-Gly (1:2)-6% OHP[5] were measured to calculate the IAST selectivity, as shown in Figure S7-8. The absorption capacities of EaCl-Gly (1:2)-6% OHP[5] for N_2 and CO_2 were 0.035 mmol/g and 0.129 mmol/g at 298.2 K and 1.0 bar, respectively. This shows that EaCl-Gly (1:2)-6% OHP[5] has a good selectivity of NH_3/CO_2 and NH_3/N_2. Moreover, the comparison results of EaCl-Gly (1:2)-6% OHP[5] with other absorbents are also listed in Table 2. It is found that the absorption capacity of CO_2 on EaCl-Gly (1:2)-6% OHP[5] was extremely low, and the selectivity of NH_3/CO_2 could reach 275 at 313.2 K and 100 kPa. The NH_3/CO_2 selectivity of EaCl-Gly (1:2)-6% OHP[5] exceeded those of many DESs and functionalized ionic liquids. Therefore, EaCl-Gly (1:2)-6% OHP[5] showed a good application potential for recovering ammonia in waste gas containing CO_2.

Table 1
Comparison of NH_3 absorption capacity for OHP[5]-based DES and other absorbents in the literature.

Entry	Samples	Temperature (K)	NH_3 absorption capacity (mmol/g) 10 kPa	100 kPa	Ref.
1	EaCl-Gly(1:2)-6% OHP[5]	298.2	2.39	10.84	This work
2	EaCl-Urea(1:1)-6% OHP[5]	313.2	0.99	4.95	This work
3	EaCl-AA(1:1)-6% OHP[5]	313.2	0.99	4.64	This work
4	EaCl + Gly (1:2)	298.2	1.59	9.34	[32]
5	EaCl + AA (1:1)	313.2	0.63	4.00	[33]
6	EaCl + Urea (1:1)	313.2	0.61	4.52	[34]
7	ChCl + TetrZ + EG (3:7:14)	298.2	6.79	13.69	[35]
8	$[Emim]_2[Co(NCS)_4]$	303.2	3.06	10.59	[20]
9	[Bim][SCN]	303.2	2.12	13.63	[36]
10	ChCl + PhOH + EG (1:5:4)	298.2	2.63	9.62	[37]
11	Tri + Gly (1:3)	313.2	–	6.71	[38]
12	[DMEA][Ac]	298.2	–	5.87	[39]
13	$[EtOHmim][BF_4]$	313.2	–	2.64	[16]
14	$[Bmim][PF_6]$	298.2	–	1.23	[40]
15	$[Li\text{-}TEG][Tf_2N]$	313.2	–	7.69	[41]
16	3,4-DHBA + EG (1:3)	298.2	5.64	11.69	[42]
17	[DEA]Cl	298.2	5.64	10.77	[43]

3.6. NH_3 absorption mechanism

In order to better describe the NH_3 absorption mechanism, the interaction between EaCl-Gly (1:2)-6% OHP[5] and NH_3 molecules was further analyzed by ^1H NMR and FTIR spectra characterization. As shown in Fig. 5, EaCl-Gly (1:2)-6% OHP[5] showed proton peaks at 4.49, 7.96 and 8.48 ppm, which were attributed to the hydroxyl group of

Table 2
NH_3/CO_2 selectivity on supramolecular-based ternary DESs and other absorbents.

Absorbent	T (K)	Absorption capacity (mmol/g)[a]		NH_3/CO_2 selectivity	Ref.
		NH_3	CO_2		
EaCl-Gly(1:2)-6% OHP[5]	298.2	10.84	0.129	84	This work
EaCl-Gly(1:2)-6% OHP[5]	313.2	6.87	0.025	275	This work
$[Emim]_2[Co(NCS)_4]$	303.2	11.70	0.223	52	[20]
$[Bmim]_2[CuCl_4]$	303.2	10.10	0.202	50	[19]
$[EtOHmim][PF_6]$	313.2	2.48	0.039	63	[16]
$[EtOHmim][BF_4]$	313.2	3.07[c]	0.050	61	[16]
NH_4SCN/CL (1:3)	313.2	1.73	0.060	29	[44]
$[Im][NO_3]/EG$ (1:3)	313.2	3.21[d]	0.023[d]	140	[12]
Im/Res (1:1)	313.2	9.06	0.189	47.9	[45]
Im/Gly (1:3)	313.2	5.81	0.156	37.3	[38]
$[Bmim][MeSO_3]/Urea$ (1:1)	313.2	0.55[e]	0.059	9.3	[46]

a: at 100 kPa. b: at 107.91 kPa. d: at 115.56 kPa. d: molar ratios. e: the absorption capacity is calculated according to the Henry's constants in original publication.

Gly, the protonated amine group of EaCl and the phenol hydroxyl group of OHP[5], respectively. These three types of proton peaks were together shifted to 5.19 ppm, while the other proton peaks of OHP[5]-based ternary DESs did not change significantly after absorption of NH_3. This suggests that the active proton hydrogen (4.49, 7.96 and 8.48 ppm) is the site of interaction with NH_3, which has been reported in previous reported literature [24,37]. Moreover, Fig. 6 shows the FTIR spectra of EaCl-Gly (1:2)-6% OHP[5] before and after NH_3 absorption. After the absorption of NH_3, the absorption peak at 1426 cm^{-1} for the in-plane bending vibration of hydroxyl group (–OH) disappeared, which is probably because the interaction between Gly and NH_3 molecules would destroy the hydrogen bonding network in Gly. Also, the absorption peak at 1513 cm^{-1} for the benzene ring skeleton vibration in OHP[5] obviously weaken after NH_3 absorption, confirming the interaction between OHP[5] and NH_3 molecules [19].

3.7. Thermodynamic study

In order to further analyze the thermal effect of supramolecular OHP [5]-based ternary DES on NH_3 absorption, the thermodynamic analysis of EaCl-Gly (1:2)-6% OHP[5] was carried out. The absorption data were fitted according to the empirical formula, as shown in Eqs. 1–3 [47].

$$q = q_{chem} + q_{phy} = q_m \frac{KP}{1+KP} + \frac{P}{H} \quad (1)$$

$$q_{chem} = q_m \frac{KP}{1+KP} \quad (2)$$

$$q_{phy} = \frac{P}{H} \quad (3)$$

Where q is the total NH_3 absorption capacity (mmol/g), q_{chem} is the chemical absorption capacity ($mmol \cdot g^{-1}$), q_{phy} is the physical absorption capacity ($mmol \cdot g^{-1}$), K is the chemical absorption equilibrium constant (kPa^{-1}), H is the Henry coefficient ($kPa \cdot g \cdot mmol^{-1}$), and q_m is the maximum absorption capacity of chemical absorption ($mmol \cdot g^{-1}$).

As shown in Fig. 7, the isotherm data of NH_3 absorption by EaCl-Gly (1:2)-6% OHP[5] fitted very well with the empirical formula, and the relevant thermodynamically fitted parameters are listed in Table S3. It can be seen that the absorption capacity of NH_3 was mainly contributed by chemical absorption in the pressure range of 0 ~ 20 kPa and the chemical absorption capacity can be negligible in the pressure range of 20 ~ 100 kPa. By contrast, the physical absorption capacity was linearly related to the NH_3 partial pressure. Subsequently, the enthalpies of chemical absorption and physical dissolution were calculated from Eqs. S3 and S4, respectively. As shown in Figure S9, the enthalpies value of $\triangle H_{chem}$ and $\triangle H_{phy}$ were −30.13 kJ/mol (Figure S9a) and −12.69 kJ/mol (Figure S9b), respectively. This finding demonstrate the presence of two kinds of interactions between EaCl-Gly (1:2)-6% OHP[5] and NH_3.

3.8. Cycle performance of OHP[5]-based ternary DES

Cycle performance is another important parameter for evaluating the property of absorbents. Therefore, the cycle performance of EaCl-Gly (1:2)-6% OHP[5] was tested for nine NH_3 absorption–desorption cycles as shown in Fig. 8. It can be seen that EaCl-Gly (1:2)-6% OHP[5] lost

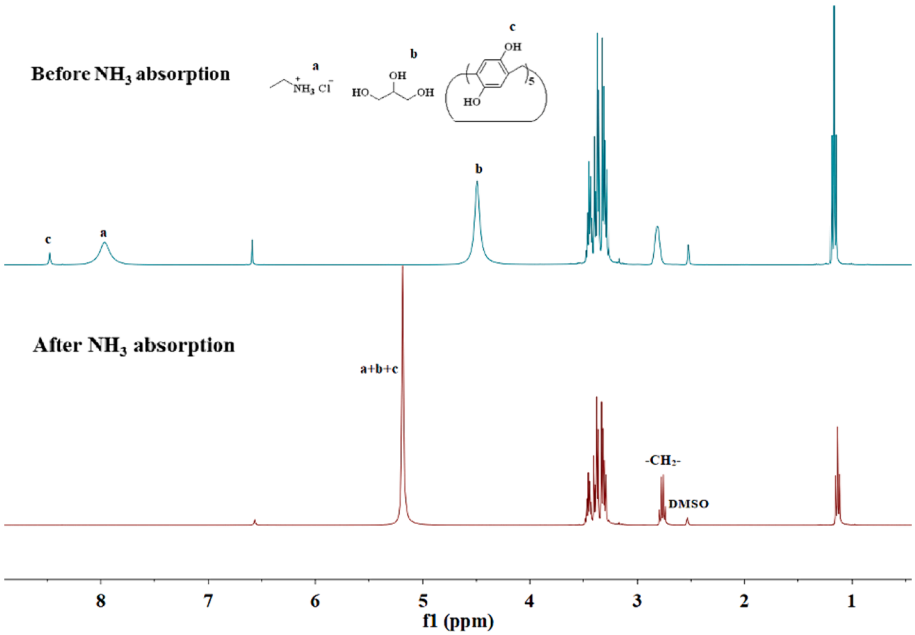

Fig. 5. ^1H NMR spectra of EaCl-Gly (1:2)-6% OHP[5] before and after NH_3 absorption.

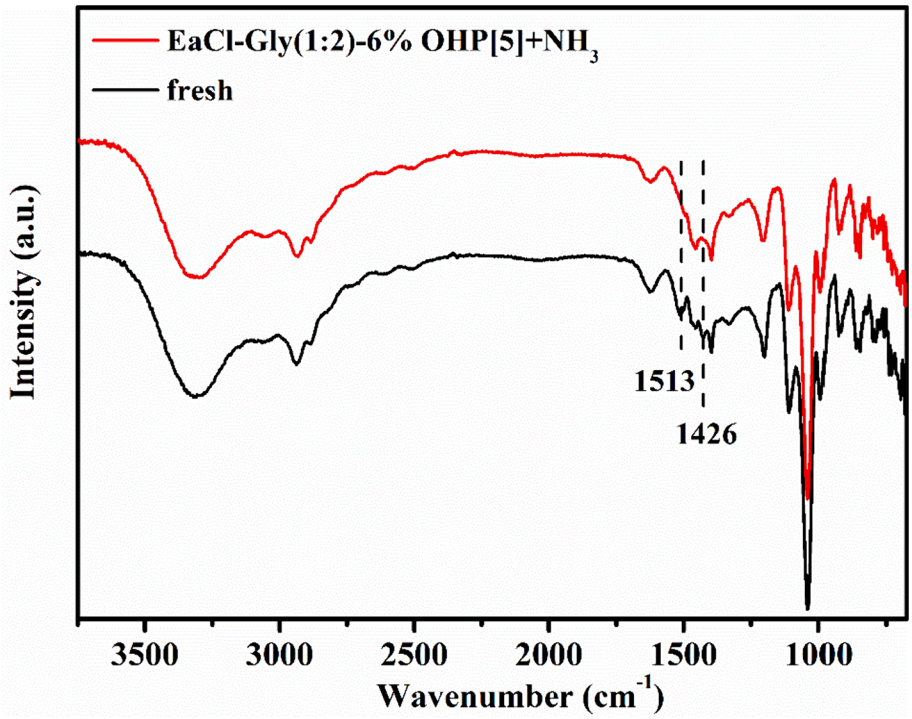

Fig. 6. FTIR spectra of EaCl-Gly (1:2)-6% OHP[5] before and after NH_3 absorption.

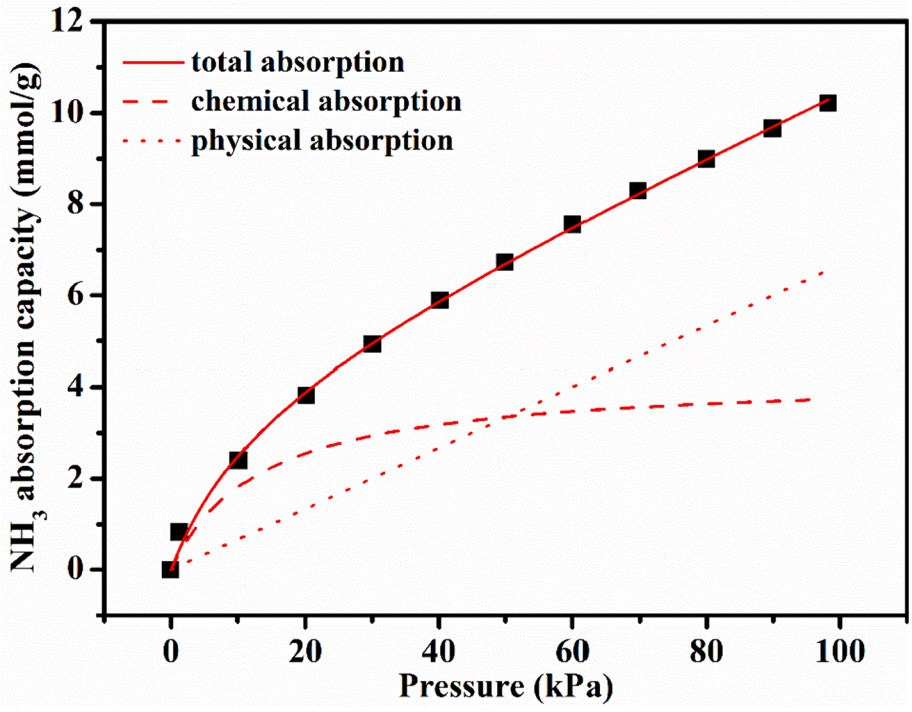

Fig. 7. Total, physical and chemical adsorption capacity of NH_3 on EaCl-Gly (1:2)-6% OHP[5].

approximately 5 ~ 7 % saturated NH_3 absorption capacity after 9 cycles. This may be because the residual NH_3 is hard to desorb and release at the desorption temperature of 353.2 K. Except for the residual fraction, the available NH_3 absorption capacity of EaCl-Gly (1:2)-6% OHP[5] can remain stable and have no obvious decrease during 9 absorption–desorption cycles, indicating a relatively good reusability of EaCl-Gly (1:2)-6% OHP[5].

4. Conclusions

In conclusion, three supramolecular-based ternary DESs were successfully prepared to realize efficient and selective absorption of NH_3. The results showed that the supramolecular-based ternary DES EaCl-Gly (1:2)-6% OHP[5] had an excellent NH_3 absorption capacity of 10.84 mmol/g and an NH_3/CO_2 selectivity of 275 at 313.2 K and 100 kPa. And the NH_3 absorption behavior and mechanism on EaCl-Gly (1:2)-6% OHP

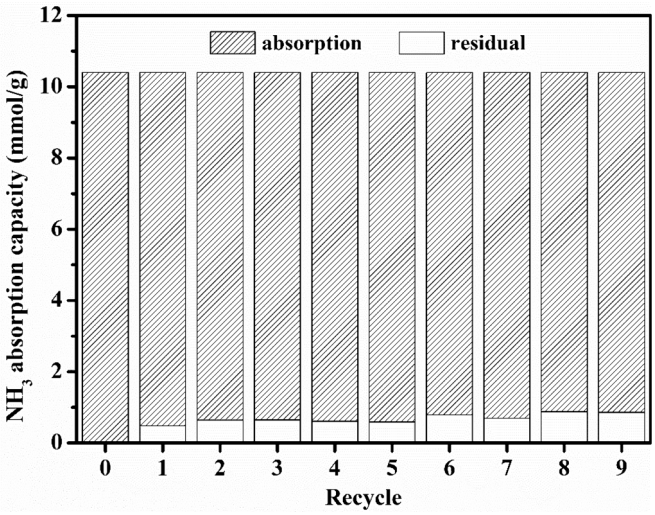

Fig. 8. Recycling of NH_3 absorption–desorption by EaCl-Gly (1:2)-6% OHP[5].

[5] was clearly illustrated by the characterizations of ^1H NMR and FTIR spectra and thermodynamic study. In addition, EaCl-Gly (1:2)-6% OHP [5] showed a good cycle stability during nine NH_3 absorption–desorption cycles. The supramolecular-based ternary DESs show excellent application prospects for recovery and utilization of ammonia resources.

CRediT authorship contribution statement

Wen-Qiang Gong: Writing – original draft, Methodology, Investigation, Data curation. **Ming-Shuai Sun:** Writing – review & editing, Methodology. **Jun Li:** Resources, Methodology. **Qiu-Ping Gong:** Resources, Methodology. **Yu-Xuan Fu:** Resources, Methodology. **Yan Zhou:** Resources, Methodology. **Duan-Jian Tao:** Writing – review & editing, Supervision, Resources, Conceptualization.

Declaration of competing interest

The authors declare that they have no known competing financial interests or personal relationships that could have appeared to influence the work reported in this paper.

Data availability

Data will be made available on request.

Acknowledgments

The project was financially supported by the Key Lab of Fluorine and Silicon for Energy Materials and Chemistry of Ministry of Education, Jiangxi Normal University (KFSEMC-202209) and the National Natural Science Foundations of China (22378178).

Appendix A. Supplementary material

Supplementary data to this article can be found online at https://doi.org/10.1016/j.molliq.2024.124505.

References

[1] L.J. Xu, C.C. Shi, Z.J. He, H. Zhang, M.Y. Chen, Z. Fang, Y. Zhang, Recent advances of producing biobased N-containing compounds via thermo-chemical conversion with ammonia process, energ, Fuel. 34 (2020) 10441–10458.
[2] X. Zhang, E.A. Davidson, D.L. Mauzerall, T.D. Searchinger, P. Dumas, Y. Shen, Managing nitrogen for sustainable development, Nature 528 (2015) 51–59.
[3] B. Pan, S.K. Lam, A. Mosier, Y. Luo, D. Chen, Ammonia volatilization from synthetic fertilizers and its mitigation strategies: a global synthesis, Agr. Ecosyst. Environ. 232 (2016) 283–289.
[4] A. Valera-Medina, H. Xiao, M. Owen-Jones, W.I.F. David, P.J. Bowen, Ammonia for power, Prog. Energ. Combust. 69 (2018) 63–102.
[5] C. Zamfirescu, I. Dincer, Using ammonia as a sustainable fuel, J. Power Sources 185 (2008) 459–465.
[6] Y. Kojima, M. Yamaguchi, Ammonia storage materials for nitrogen recycling hydrogen and energy carriers, Int. J. Hydrogen Energ. 45 (2020) 10233–10246.
[7] J.W. Erisman, A. Bleeker, J. Galloway, M.S. Sutton, Reduced nitrogen in ecology and the environment, Environ. Pollut. 150 (2007) 140–149.
[8] M. Van Damme, L. Clarisse, S. Whitburn, J. Hadji-Lazaro, D. Hurtmans, C. Clerbaux, P.F. Coheur, Industrial and agricultural ammonia point sources exposed, Nature 564 (2018) 99–103.
[9] J. Fernandez-Seara, J. Sieres, The importance of the ammonia purification process in ammonia-water absorption systems, energ. convers, Manage. 47 (2006) 1975–1987.
[10] G.M. Bernd Rumpf, Solubility of ammonia in aqueous solutions of phosphoric acid: model development and application, J. Solution Chem. 23 (1994) 37–51.
[11] B. Rumburg, M. Neger, G.H. Mount, D. Yonge, J. Filipy, J. Swain, R. Kincaid, K. Johnson, Liquid and atmospheric ammonia concentrations from a dairy lagoon during an aeration experiment, Atmos. Environ. 38 (2004) 1523–1533.
[12] Y.K. Cao, X.P. Zhang, S.J. Zeng, Y.R. Liu, H.F. Dong, C. Deng, Protic ionic liquid-based deep eutectic solvents with multiple hydrogen bonding sites for efficient absorption of NH_3, AIChE J. 66 (2020) e16253.
[13] D.W. Shang, X.P. Zhang, S.J. Zeng, K. Jiang, H.S. Gao, H.F. Dong, Q.Y. Yang, S. J. Zhang, Protic ionic liquid [Bim][NTf2] with strong hydrogen bond donating ability for highly efficient ammonia absorption, Green Chem. 19 (2017) 937–945.
[14] P.F. Li, D.W. Shang, W.H. Tu, S.J. Zeng, Y. Nie, L. Bai, H.F. Dong, X.P. Zhang, NH_3 absorption performance and reversible absorption mechanisms of protic ionic liquids with six-membered N-heterocyclic cations, Sep. Purif. Technol. 248 (2020) 117087.
[15] B.B. Yang, D.W. Shang, W.H. Tu, S.J. Zeng, L. Bai, H. Wang, X.P. Zhang, Studies on the physical properties variations of protic ionic liquid during NH_3 absorption, J. Mol. Liq. 296 (2019) 111791.
[16] Z.J. Li, X.P. Zhang, H.F. Dong, X.C. Zhang, H.S. Gao, S.J. Zhang, J.W. Li, C. M. Wang, Efficient absorption of ammonia with hydroxyl functionalized ionic liquids, RSC Adv. 5 (2015) 81362–81370.
[17] L. Yuan, H.S. Gao, H.Y. Jiang, S.J. Zeng, T. Li, B.Z. Ren, X.P. Zhang, Experimental and thermodynamic analysis of NH_3 absorption in dual-functionalized pyridinium-based ionic liquids, J. Mol. Liq. 323 (2021) 114601.
[18] L. Yuan, X.P. Zhang, B.Z. Ren, Y.L. Yang, Y.G. Bai, L. Bai, H.S. Gao, S.J. Zeng, Dual-functionalized protic ionic liquids for efficient absorption of NH_3 through synergistically physicochemical interaction, J. Chem. Technol. Biot. 95 (2020) 1815–1824.
[19] J.L. Wang, S.J. Zeng, F. Huo, D.W. Shang, H.Y. He, L. Bai, X.P. Zhang, J.W. Li, Metal chloride anion-based ionic liquids for efficient separation of NH_3, J. Clean. Prod. 206 (2019) 661–669.
[20] S.J. Zeng, L. Liu, D.W. Shang, J.P. Feng, H.F. Dong, Q.X. Xu, X.P. Zhang, S.J. Zhang, Efficient and reversible absorption of ammonia by cobalt ionic liquids through lewis acid-base and cooperative hydrogen bond interactions, Green Chem. 20 (2018) 2075–2083.
[21] D.W. Shang, S.J. Zeng, X.P. Zhang, X.C. Zhang, L. Bai, H.F. Dong, Highly efficient and reversible absorption of NH_3 by dual functionalised ionic liquids with protic and lewis acidic sites, J. Mol. Liq. 312 (2020) 113411.
[22] N.N. Cheng, Z.L. Li, H.C. Lan, W.L. Xu, K. Huang, Remarkable NH_3 absorption in metal-based deep eutectic solvents by multiple coordination and hydrogen-bond interaction, AIChE J. 68 (2022) e17660.
[23] X.X. Sun, Q.H. Wang, S.H. Wu, X.Y. Zhao, L.G. Wei, K.L. Li, J.A. Hao, L. Wei, S. R. Zhai, Q.D. An, Metal chlorides-promoted ammonia absorption of deep eutectic solvent, Int. J. Hydrogen Energ. 47 (2022) 16121–16131.
[24] Y.D. Ma, J.Y. Zhang, K. Huang, L.L. Jiang, Highly efficient and selective separation of ammonia by deep eutectic solvents through cooperative acid-base and strong hydrogen-bond interaction, J. Mol. Liq. 337 (2021) 116463.
[25] N.L. Strutt, H.C. Zhang, S.T. Schneebeli, J.F. Stoddart, Functionalizing pillar[n] arenes, Acc. Chem. Res. 47 (2014) 2631–2642.
[26] N. Song, T. Kakuta, T.A. Yamagishi, Y.W. Yang, T. Ogoshi, Molecular-scale porous materials based on pillar[n]arenes, Chem 4 (2018) 2029–2053.
[27] X.F. Li, D. Feng, M.Y. Chai, S.C. Xu, A. Mohammedomar, W.B. Zhao, Efficient SO2 capture by 2-(diethylamino)ethanol/hexadecane phase separation absorbent, energ, Fuel. 34 (2020) 15039–15047.
[28] M.Y. Chai, W.B. Zhao, G.M. Li, S.C. Xu, Q.M. Jia, Y. Chen, Novel SO2 phase-change absorbent: mixture of N, N-dimethylaniline and liquid paraffin, Ind. Eng. Chem. Res. 57 (2018) 12502–12510.
[29] T. Ogoshi, T. Aoki, K. Kitajima, S. Fujinami, T.A. Yamagishi, Y. Nakamoto, Facile, rapid, and high-yield synthesis of pillar[5]arene from commercially available reagents and its X-ray crystal structure, J. Org. Chem. 76 (2011) 328–331.
[30] F.F. Chen, K. Huang, Y. Zhou, Z.Q. Tian, X. Zhu, D.J. Tao, D.E. Jiang, S. Dai, Multi-molar absorption of CO_2 by the activation of carboxylate groups in amino acid ionic liquids, Angew. Chem. Int. Ed. Engl. 55 (2016) 7166–7170.
[31] J. Fu, J.Y. Liu, G.H. Zhang, Q.H. Zhu, S.L. Wang, S. Qin, L. He, G.H. Tao, Boost of gas adsorption kinetics of covalent organic frameworks via ionic liquid solution process, Small (2023) e2302570.
[32] W.J. Jiang, F.Y. Zhong, Y. Liu, K. Huang, Effective and reversible capture of NH_3 by ethylamine hydrochloride plus glycerol deep eutectic solvents, ACS Sustain. Chem. Eng. 7 (2019) 10552–10560.

[33] J.Y. Zhang, K. Huang, Densities and viscosities of, and NH_3 solubilities in deep eutectic solvents composed of ethylamine hydrochloride and acetamide, J. Chem. Thermody. 139 (2019) 105883.
[34] J.Y. Zhang, L.Y. Kong, K. Huang, NH_3 solubilities and physical properties of ethylamine hydrochloride plus urea deep eutectic solvents, J. Chem. Eng. Data 64 (2019) 3821–3830.
[35] F.Y. Zhong, L. Zhou, J. Shen, Y. Liu, J.P. Fan, K. Huang, Rational design of azole-based deep eutectic solvents for highly efficient and reversible capture of ammonia, ACS Sustain. Chem. Eng. 7 (2019) 14170–14179.
[36] D.W. Shang, L. Bai, S.J. Zeng, H.F. Dong, H.S. Gao, X.P. Zhang, S.J. Zhang, Enhanced NH_3 capture by imidazolium-based protic ionic liquids with different anions and cation substituents, J. Chem. Technol. Biot. 93 (2018) 1228–1236.
[37] F.Y. Zhong, H.L. Peng, D.J. Tao, P.K. Wu, J.P. Fan, K. Huang, Phenol-based ternary deep eutectic solvents for highly efficient and reversible absorption of NH_3, ACS Sustain. Chem. Eng. 7 (2019) 3258–3266.
[38] D.S. Deng, X.Z. Duan, B. Gao, C. Zhang, X.X. Deng, L. Gong, Efficient and reversible absorption of NH_3 by functional azole-glycerol deep eutectic solvents, New J. Chem. 43 (2019) 11636–11642.
[39] A. Yokozeki, M.B. Shiflett, Vapor-liquid equilibria of ammonia+ionic liquid mixtures, Appl. Energ. 84 (2007) 1258–1273.
[40] A.Y.M.B. Shiflett, Ammonia solubilities in room-temperature ionic liquids, Ind. Eng. Chem. Res. 46 (2007) 1605–1610.
[41] Z.P. Cai, J.Y. Zhang, Y.D. Ma, W.Q. Wu, Y.N. Cao, K. Huang, L.L. Jiang, Chelation-activated multiple-site reversible chemical absorption of ammonia in ionic liquids, AIChE J. 68 (2022) e17632.
[42] L. Zheng, X.Y. Zhang, Q.K. Li, Y.D. Ma, Z.P. Cai, Y.N. Cao, K. Huang, L.L. Jiang, Effective ammonia separation by non-chloride deep eutectic solvents composed of dihydroxybenzoic acids and ethylene glycol through multiple-site interaction, Sep. Purif. Technol. 309 (2023) 123136.
[43] J.Y. Zhang, S.Q. Fang, L. Zheng, X. Li, Y.D. Ma, H.W. Zhang, Z.P. Cai, Y.N. Cao, K. Huang, L.L. Jiang, Evaluating diethanolammonium chloride as liquid solvent for gas separation from experiments and theoretical calculations, AIChE J. 69 (2023) e18231.
[44] D.S. Deng, B. Gao, C. Zhang, X.Z. Duan, Y.H. Cui, J.H. Ning, Investigation of protic NH_4SCN-based deep eutectic solvents as highly efficient and reversible NH_3 absorbents, Chem. Eng. J. 358 (2019) 936–943.
[45] Q. Luo, Q.H. Wang, X.X. Sun, H. Wu, J.G. Hao, L.G. Wei, S.R. Zhai, Z.Y. Xiao, Q. D. An, Dual-active-sites deep eutectic solvents based on imidazole and resorcinol for efficient capture of NH_3, Chem. Eng. J. 416 (2021) 129114.
[46] A.I. Akhmetshina, A.N. Petukhov, A. Mechergui, A.V. Vorotyntsev, A.V. Nyuchev, A.A. Moskvichev, I.V. Vorotyntsev, Evaluation of methanesulfonate-based deep eutectic solvent for ammonia sorption, J. Chem. Eng. Data 63 (2018) 1896–1904.
[47] M.A. Islam, M.A. Kalam, M.R. Khan, Reactive gas solubility in water: an empirical relation, Ind. Eng. Chem. Res. 39 (2000) 2627–2630.